Original Article

Institution of MECHANICAL ENGINEERS
Journal of ENGINEERING MANUFACTURE

Proc IMechE Part B:
J Engineering Manufacture
2015, Vol. 229(8) 1385–1394

DOI: 10.1177/0954405414535591
pib.sagepub.com
SAGE

Grey relational analysis coupled with firefly algorithm for multiobjective optimization of wire electric discharge machining

A Varun and N Venkaiah

Abstract

Complex engineering problems are often required to be addressed for multiobjective optimization. Wire electric discharge machining is one such multiobjective optimization problem. Conflicting objectives such as material removal rate, surface roughness and kerf have always been research interest for optimization. In this article, a novel optimization strategy has been formulated by coupling grey relational analysis with firefly algorithm to optimize the responses. Process parameters such as pulse-on time, pulse-off time, peak current and servo voltage are studied. Response parameters such as material removal rate, surface roughness and kerf are considered. Firefly algorithm is the main technique and grey relational analysis is used to generate a grey relational grade. This grade is further used in firefly algorithm for movement of firefly to the neighboring brighter and attractive firefly. In this process of self-organization, simultaneous optimal solution for material removal rate, surface roughness and kerf is obtained. Peak current is found to be the most influencing factor affecting all the three responses. Pareto surface plot is also plotted to recommend alternate solutions for various responses based on the priorities. As the proposed strategy is generalized, it can be customized and applied for any multiobjective optimization problem.

Keywords

Wire electric discharge machining, firefly algorithm, grey relational analysis, multiobjective optimization, hybrid method

Date received: 26 January 2014; accepted: 23 April 2014

Introduction

Wire electric discharge machining (WEDM) is constantly attracting a lot of researchers and industrialists because of its wide range of applications for machining almost any material, which can conduct. In the last 25 years, developers have been constantly improving WEDM process to meet the requirements of the industry.

Present day's manufacturing sector demands production of parts, which are of high quality without compromising on the machining speed. This is possible by proper selection of machining parameters. In the case of WEDM process, material removal rate (MRR), surface roughness (SR) and kerf are important responses, which determine the production efficiency and quality of the product. Selection of proper machining parameters is vital since it also includes interactions among them, which makes the process stochastic in nature. Since there is no single universal tool for finding the best set of machining parameters to achieve global optimum solution, researchers are constantly attempting to propose the most efficient algorithm.

Global optimality in WEDM with different conflicting objectives is not easy to reach. Many researchers have focused on achieving multiobjective optimization of WEDM. Golshan et al.[1] compared the performance of brass wire and zinc-coated brass wire and optimized multiple objectives using non-dominated sorting genetic algorithm-II (NSGA-II). Pareto optimal set of solutions is obtained for both the wires and concluded that zinc-coated brass wire was more predictable and reliable. Rao and Pawar[2] developed a mathematical model using response surface methodology (RSM) and

Department of Mechanical Engineering, National Institute of Technology Warangal, Warangal, India

Corresponding author:
N Venkaiah, Department of Mechanical Engineering, National Institute of Technology Warangal, Warangal 506004, Andhra Pradesh, India.
Email: n_venkaiah@nitw.ac.in

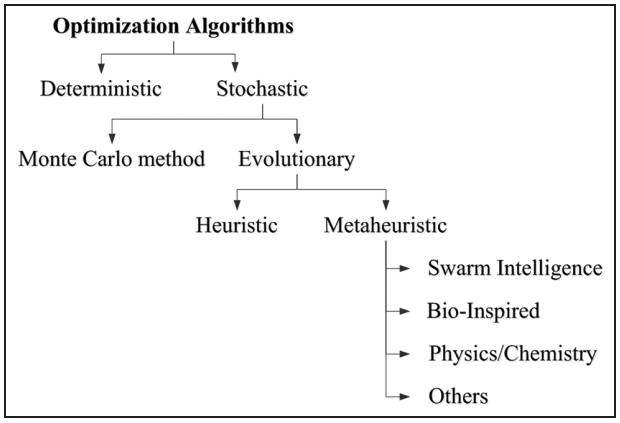

Figure 1. Classification of optimization algorithms.

optimized WEDM process parameters using artificial bee colony (ABC). Garg et al.[3] formulated multiobjective optimization problem of WEDM using Box–Behnken design and optimized using NSGA-II method. A non-dominated Pareto optimal solution set was obtained. Thereby, the best solution was selected. Most of them used Taguchi- or RSM-based design of experiments and formulated the regression equations. These regression equations serve as objective functions for optimization algorithms.

Optimization algorithms can be broadly classified as deterministic and stochastic processes, as shown in Figure 1. Furthermore, stochastic process can be branched into Monte Carlo methods and evolutionary algorithms. Heuristic and metaheuristic methods come under evolutionary algorithms.

Metaheuristic algorithms are very powerful in solving stochastic optimization problems. Many researchers have been developing new algorithms by drawing inspiration from nature.[4] These algorithms can be broadly divided into four major categories: swarm intelligence (SI) based, bio-inspired (but not SI-based), Physics/Chemistry based and others. SI-based algorithms are among the most popular and widely used. They are concerned with collective, emerging behavior of multiple, interacting agents who follow some simple rules. And they are inspired by the collective behavior of social insects, such as ants, termites, bees and fireflies, as well as from other animal societies like flocks of birds, fish and so on. The reason for such popularity is that SI algorithms usually share information among multiple agents, so that self-organization, co-evolution and learning during iterations may help to provide the high efficiency of most SI-based algorithms.

Inspired by the tropic firefly swarms and their flashing behavior, Yang[5,6] developed a new metaheuristic algorithm called firefly algorithm (FA), which is based on SI. Although the FA has many similarities with other algorithms based on the SI, this algorithm is much simpler in both concept and implementation. Furthermore, the recent literature shows that the algorithm has outperformed other well-known algorithms like genetic algorithm (GA), for solving many optimization problems. Khadwilard et al.[7] applied FA for solving job shop scheduling problem with five different benchmark datasets and concluded that FA generates better results. Aungkulanon et al.[8] compared FA and particle swarm optimization (PSO) for their processing time, convergence speed and quality of results using benchmark models. FA outperformed PSO. Bharathi Raja et al.[9] applied different optimization techniques such as simulated annealing (SA), GA, PSO, FA, hybrid algorithm (HA) and memetic algorithm (MA) for mathematical modeling of turning operation. PSO was found to give best results followed by FA. Chaiead et al.[10] compared FA and bees algorithm (BA) on execution time, accuracy and convergence criteria. FA was found to be better than BA. Bharathi Raja et al.[11] applied FA for optimization of die-sinking electric discharge machining (EDM) of hardened die steel. FA was used to predict the optimal parameters of EDM to yield SR and machining time.

In the multiobjective optimization problems, multiple objective functions conflict with one another. The aim should be to find a vector of decision variables that satisfies constraints and optimizes the objective functions.[12] In grey relational analysis (GRA), the responses are first normalized in the range of 0 to 1. Next, based on the normalized data, grey relational coefficients are calculated. Entropy-based weights are employed to determine the relative weighting factors for each output response. Then, overall grey relational grade (GRG) is determined by averaging the grey relational coefficients corresponding to selected responses.[13]

Methodology

In this article, a face-centered central composite design (FCCD) is applied for experimentation. The responses considered are MRR, SR and kerf. Analysis of variance (ANOVA) is performed and regression modeling is carried out to generate the objective functions for the output responses. FA is used for multiobjective optimization of the objective functions. Based on the fitness values, GRG is computed using GRA in each iteration. FA uses this GRG, and search is made to achieve higher GRG. The highest GRG corresponds to global optimal solution in the selected range of process parameters. Figure 2 depicts the steps involved in the proposed methodology.

Multiobjective FA

The FA has been designed to address all varieties of optimization problems. However, all algorithms usually pose some limitations, as stated in the No Free Lunch theorem.[14] In order to overcome these limitations, hybrid methods are developed to seek improvements.

FA tries to mimic the tropical fireflies, attraction behavior and flashing pattern. Researchers identified that the purpose of this flashing lights is mainly to

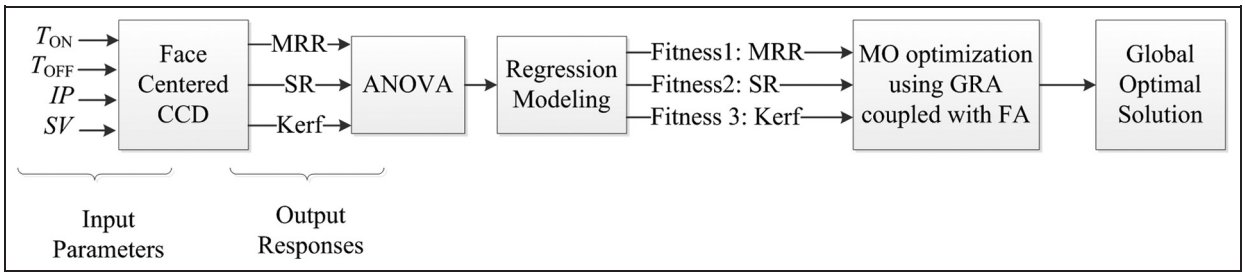

Figure 2. Steps in proposed methodology.
T_{ON}: pulse-on time; T_{OFF}: pulse-off time; IP: peak current; SV: servo voltage; CCD: central composite design; ANOVA: analysis of variance; MRR: material removal rate; SR: surface roughness; MO: multiobjective; GRA: grey relational analysis; FA: firefly algorithm.

attract their mating partners and at the same time to warn potential threat from predators. Yang[5] developed FA based on few rules obeyed by fireflies:

- Fireflies are unisex so that one firefly will be attracted to other fireflies regardless of their sex.
- The attractiveness is proportional to the brightness, and they both decrease as their distance increases. Thus, for any two flashing fireflies, the less brighter one will move toward the brighter one. If there is no brighter one, then a particular firefly moves randomly.
- The brightness of a firefly is determined by the landscape of the objective function.

This population-based FA finds the global optima based on SI. In this work, initialized agents or fireflies are randomly distributed in the search space based on the objective function generated from regression modeling. The key modification in this article is that a GRG is calculated based on the fitness values of the individual objective functions. The methodology is explained in detail in section "GRA." Then search is made to achieve higher GRG using FA.

The firefly emits light proportional to the value of GRG. The variation of light intensity and formulation of attractiveness are the two important phenomena for the co-evolution of FA.[4] The brightness I of a firefly at a particular location x can be chosen as $I(x) \propto f(x)$, which means brightness is proportional to the value of the objective function. However, the attractiveness β is relative and varies with the distance r_{ij} between firefly i and firefly j. As the distance increases from source of light, its intensity decreases as absorbed by the medium. Hence, the attractiveness varies with the degree of absorption. The attractiveness of a firefly can be represented as a monotonically decreasing function[6] given by equation (1)

$$\beta(r) = \beta_0 \, e^{(-\gamma r^m)} \tag{1}$$

where r is the distance between any two fireflies, β_0 is the initial attractiveness at $r = 0$ and γ is an absorption coefficient, which controls the light intensity.

The distance between any two fireflies i and j, at position x_i and x_j, respectively, can be defined as a Cartesian or Euclidean distance as follows

$$r_{ij} = \left\| x_i - x_j \right\| = \sqrt{\sum_{k=1}^{d} \left(x_{i,k} - x_{j,k} \right)^2} \tag{2}$$

where $x_{i,k}$ is the kth component of the spatial coordinate x_i of the ith firefly and d is the number of dimensions.

The movement of a firefly i, which is attracted by a brighter firefly j, is given by equation (3)

$$x_i = x_i + \beta_0 e^{-\gamma r_{ij}^2} (x_i - x_j) + \alpha \left(rand - \frac{1}{2} \right) \tag{3}$$

where the first term is the current position of a firefly, the second term denotes firefly's attractiveness to light intensity seen by adjacent fireflies and the third term is used for the random movement of a firefly when there are no brighter ones. The coefficient α is a randomization parameter determined by the problem of interest, while *rand* is a random number generator uniformly distributed in the space [0, 1]. $\beta_0 = 1.0$ and the attractiveness or absorption coefficient, $\gamma = 1.0$, are used for quick convergence.[15]

Solving multiobjective optimization problem is important for addressing majority of engineering problems. FA can be used to solve multiobjective optimization problems by combining all the output response objectives into single objective. Apostolopoulos and Aristidis[12] implemented weighted sum method in FA for combining multiple objectives into a single objective optimization problem. In this work, FA is coupled with GRA to combine multiobjective WEDM output responses into a single GRG.

GRA

Deng[16] proposed GRA to deal with uncertain and incomplete systems. GRA is gaining popularity in the recent years because of its ability to determine multiple performance measures. Relative weighting for each attribute is found using entropy weighting method.[17] Entropy is originally a thermodynamic concept.

Information represents ordered degree, but entropy represents disordered degree of system in information theory.[18] According to which, the objective with higher variation in its objective function values should be assigned a higher weightage.

Objective fitness values generated by the FA are used to obtain GRG. GRG is defined as the relative degree between sequence of individual responses. One sequence $x_i^*(k)$ selected as the reference sequence is called the localized GRG, that is, one sequence exists in the grey relation space $\{P(X); \Gamma\}$

$$x_i(k) = (x_i(1), x_i(2), \ldots, x_i(k)) \in X$$

where $i = 0, 1, 2, \ldots, m \in N$; $k = 1, 2, \ldots, n \in N$, that is

$$x_0(k) = (x_0(1), x_0(2), \ldots, x_0(k))$$
$$x_1(k) = (x_1(1), x_1(2), \ldots, x_1(k))$$
$$\vdots$$
$$x_m(k) = (x_m(1), x_m(2), \ldots, x_m(k))$$

Fitness values of objective functions from FA are considered as the sequence to be used for finding GRG. In GRA, initially normalization of data is performed. This is also called as grey relational generation. The normalized objective fitness results, x_i, can be expressed as

Larger-the-better (LB)

$$x_i^*(k) = \frac{x_i^0(k) - \min x_i^0(k)}{\max x_i^0(k) - \min x_i^0(k)} \tag{4}$$

Smaller-the-better (SB)

$$x_i^*(k) = \frac{\max x_i^0(k) - x_i^0(k)}{\max x_i^0(k) - \min x_i^0(k)} \tag{5}$$

where $x_i^*(k)$ is the value after the grey relational generation process and $\min x_i^0(k)$ and $\max x_i^0(k)$ denote the minimum and maximum of $x_i^0(k)$, respectively.

Entropy weighting is introduced as follows:

1. Each attribute summation, D_k, is computed

$$D_k = \sum_{i=1}^{m} x_i(k) \tag{6}$$

2. Normalization coefficient, K, is computed

$$K = \frac{1}{0.6487 \times n} \tag{7}$$

where n represents the number of responses.

3. Entropy for specific attribute, e_k, is found

$$e_k = K \sum_{i=1}^{m} W_e(Z_i) \tag{8}$$

where $W_e(Z_i) = Z_i e^{(1-Z_i)} + (1 - Z_i) e^{Z_i} - 1$ and

$$Z_i = \frac{x_i(k)}{D_k}$$

4. Total entropy value, E, is given by

$$E = \sum_{k=1}^{n} e_k \tag{9}$$

5. Relative weighting factor, λ_k, is given by

$$\lambda_k = \frac{1}{n - E} |(1 - e_k)| \tag{10}$$

According to the grey relational generation and weighting factor of each attribute, GRG, Γ, is given by

$$\Gamma_j = \frac{\Delta_{\min} + \Delta_{\max}}{\Delta'_j + \Delta_{\max}} \tag{11}$$

where $i = 0, 1, 2, \ldots\ldots, n$; $k = 1, 2, \ldots\ldots, m, j \in i$ and

$$\Delta'_j = \frac{1}{n} \sum_{i=1}^{n} \Delta_{0i}(k), \quad \Delta_{0i}(k) = |x_0(k) - x_i(k)|$$

$\Delta_{\min}$ and $\Delta_{\max}$ are constants as given by

$$\Delta_{\min} = \forall^{\min} j \in \forall^{\min} k \left| x_0(k) - x_j(k) \right|$$
$$\Delta_{\max} = \forall^{\max} j \in \forall^{\max} k \left| x_0(k) - x_j(k) \right|$$

The overall performance characteristic of the multiple response process depends upon the calculated GRG. Therefore, GRG is used in the FA for movement of firefly to the brighter and attractive firefly. With this hybrid method, multiobjective optimization is attempted in this work.

The pseudo-code for proposed hybrid method called GRA coupled with FA is presented in Table 1. The procedure starts by considering formulated regression equation as the objective function. Initially, population of n fireflies is distributed among the search space uniformly. Once the fixed number of iterations and limits of search space are defined, the iterations start to evaluate each of the responses individually. Then, GRA is carried out in each iteration, and a combined GRG is calculated using entropy weighting method as described in section "GRA." Then, the co-evolution of the fireflies continues by moving toward the attractive fireflies as illustrated in section "Multiobjective FA."

Experimental procedure

WEDM experiments were conducted on an ULTRACUT S1 machine. The controllable process parameters are selected based on the trial experiments carried out using one-factor-at-a-time approach; care is taken to see that the parameter ranges are well within the working range of machine without wire breakage.

In this work, experiments are carried out by adopting RSM to study the effect of the input parameters presented in Table 2. Four process parameters at three levels are selected, and a FCCD is adopted for conducting

Table 1. Pseudo-code.

Objective functions $f_1(x), \ldots, f_k(x)$ with $x = (x_1, x_2, \ldots, x_d)^T$, d = no. of design variables
Generate an initial population of fireflies randomly x_i ($i = 1, 2, \ldots, n$) where n = no. of fireflies.
Light intensity I at x is determined by $f(x)$ for all fireflies.
While ($i <$ MaxGen)
  Evaluate individual responses $f_1(x), \ldots, f_k(x)$
  Generate grey relational generation
  Generate grey relational grade based on the entropy method
  For $i = 1$ to n
    For $j = 1$ to n
      If ($I > J$), move i toward j
        Calculate attractiveness β and distance r_{ij}
        Update variables and pass to the next iterations
      End if
    End for j
  End for i
  Rank fireflies in order and find the best firefly so far.
End while
Post-process results and visualization.

Table 2. Process parameters and their levels.

Process parameters	Unit	Levels		
		1	2	3
A. Pulse-on time (T_{ON})	μs	105	110	115
B. Pulse-off time (T_{OFF})	μs	50	55	60
C. Peak current (IP)	A	10	11	12
D. Servo voltage (SV)	V	10	50	90

the experiments. Twenty-six runs with two center points are executed, and their observations have been fitted to the second-order polynomial model. Output responses such as MRR, SR and kerf are studied. A zinc-coated copper wire with 0.25 mm diameter is used. The material selected is EN 353, which is a case-carburized steel. This material has various applications including crown wheel, crown pinion and pinion shaft. Machining time for a length of 5 mm slot is recorded for each workpiece. Thickness of the workpiece is 10 mm. The observations are presented in Table 3.

Table 3. Experimental layout.

Serial number	Type	T_{ON} (μs)	T_{OFF} (μs)	IP (A)	SV (V)	MRR (mm^3/min)	SR (μm)	Kerf (mm)
1	Factorial	105	50	10	10	0.156	3.65	0.311
2	Factorial	115	50	10	10	0.201	3.62	0.306
3	Factorial	105	60	10	10	0.199	2.14	0.327
4	Factorial	115	60	10	10	0.201	3.35	0.313
5	Factorial	105	50	12	10	4.754	2.05	0.348
6	Factorial	115	50	12	10	8.553	3.2	0.344
7	Factorial	105	60	12	10	3.478	1.81	0.325
8	Factorial	115	60	12	10	6.658	3.15	0.407
9	Factorial	105	50	10	90	0.287	5.2	0.352
10	Factorial	115	50	10	90	0.278	4.88	0.347
11	Factorial	105	60	10	90	0.2	6.5	0.345
12	Factorial	115	60	10	90	0.223	5.55	0.358
13	Factorial	105	50	12	90	1.405	3.18	0.378
14	Factorial	115	50	12	90	5.114	2.35	0.431
15	Factorial	105	60	12	90	1.227	2.35	0.373
16	Factorial	115	60	12	90	1.981	1.6	0.449
17	Axial	105	55	11	50	2.385	1.58	0.352
18	Axial	115	55	11	50	6.754	2.3	0.412
19	Axial	110	50	11	50	5.482	1.74	0.394
20	Axial	110	60	11	50	3.869	1.52	0.392
21	Axial	110	55	10	50	0.432	2.45	0.352
22	Axial	110	55	12	50	6.448	2.23	0.393
23	Axial	110	55	11	10	7.673	1.6	0.368
24	Axial	110	55	11	90	2.309	1.96	0.401
25	Center	110	55	11	50	5.89	2.15	0.39
26	Center	110	55	11	50	6.164	1.7	0.385

T_{ON}: pulse-on time; T_{OFF}: pulse-off time; IP: peak current; SV: servo voltage; SR: surface roughness; MRR: material removal rate.

Table 4. ANOVA and *F*-test for MRR.

Serial number	Process parameters	Degrees of freedom	Sum of squares	Mean square	*F*-test	*p*-value (prob > *F*)	Percentage of contribution
1	A—T_{ON}	1	13.99558	13.99558	10.28656	0.0083	6.981394
2	B—T_{OFF}	1	3.730091	3.730091	2.741567	0.1260	1.860676
3	C—IP	1	77.87936	77.87936	57.24029	< 0.0001	38.84845
4	D—SV	1	19.73804	19.73804	14.5072	0.0029	9.845902
5	AB	1	0.803264	0.803264	0.590388	0.4584	0.400691
6	AC	1	8.095448	8.095448	5.950046	0.0329	4.038241
7	AD	1	0.406088	0.406088	0.298469	0.5958	0.202568
8	BC	1	2.546418	2.546418	1.871583	0.1986	1.270226
9	BD	1	0.006602	0.006602	0.004852	0.9457	0.003293
10	CD	1	12.15743	12.15743	8.935545	0.0123	6.064472
11	A^2	1	1.146274	1.146274	0.842496	0.3784	0.571794
12	B^2	1	0.811819	0.811819	0.596676	0.4561	0.404958
13	C^2	1	8.283957	8.283957	6.088598	0.0313	4.132275
14	D^2	1	0.156906	0.156906	0.115324	0.7406	0.078269
15	Residual	11	14.96626	1.360569			
16	Lack of fit	10	14.92872	1.492872	39.76962	0.1228	7.446873
17	Pure error	1	0.037538	0.037538			0.018725
18	Cor. total	25	200.4696				100

T_{ON}: pulse-on time; T_{OFF}: pulse-off time; IP: peak current; SV: servo voltage; Cor. total: Corrected Total.

Table 5. ANOVA and *F*-test for SR.

Serial number	Process parameters	Degrees of freedom	Sum of squares	Mean square	*F*-test	*p*-value (prob > *F*)	Percentage of contribution
1	A—T_{ON}	1	0.131756	0.131756	0.337506	0.5730	0.286593
2	B—T_{OFF}	1	0.200556	0.200556	0.513744	0.4885	0.436246
3	C—IP	1	13.2098	13.2098	33.83828	0.0001	28.73378
4	D—SV	1	4.5	4.5	11.52722	0.0060	9.78834
5	AB	1	0.0484	0.0484	0.123982	0.7314	0.105279
6	AC	1	0.0625	0.0625	0.1601	0.6967	0.135949
7	AD	1	2.6569	2.6569	6.805927	0.0243	5.779254
8	BC	1	0.265225	0.265225	0.679402	0.4273	0.576914
9	BD	1	0.378225	0.378225	0.968863	0.3461	0.82271
10	CD	1	6.375625	6.375625	16.33183	0.0019	13.86817
11	A^2	1	0.568129	0.568129	1.455323	0.2530	1.235787
12	B^2	1	0.066383	0.066383	0.170047	0.6880	0.144396
13	C^2	1	1.942861	1.942861	4.976841	0.0475	4.226086
14	D^2	1	0.2477	0.2477	0.63451	0.4426	0.538794
15	Residual	11	4.294184	0.39038			
16	Lack of fit	10	4.192934	0.419293	4.141169	0.3663	9.120414
17	Pure error	1	0.10125	0.10125			0.220238
18	Cor. total	25	45.97307				100

T_{ON}: pulse-on time; T_{OFF}: pulse-off time; IP: peak current; SV: servo voltage; Cor. total: Corrected Total.

ANOVA

ANOVA and *F*-test were performed for studying the statistically significant process parameters, and the percent contribution of these parameters are also shown in Tables 4–6. ANOVA results for MRR listed in Table 4 show that *p*-value, which are less than 0.05, indicates that null hypothesis should be rejected, and thus, the effect of the respective factor is significant. It can be seen from Table 4 that the pulse-on time (T_{ON}), peak current (IP), servo voltage (SV), $T_{ON} \times IP$, $IP \times SV$ and IP^2 have most significant impact on MRR. Regression analysis is also performed to find the relationship between factors and MRR. The R^2 is given as 0.9253 and adjusted R^2 is 0.8303. R^2 value indicates that the predictors explain 92.5% of the variance in MRR and the adjusted R^2 accounts for the number of predictors in the model. Regression equation for MRR is given in equation (12)

$$\begin{aligned} MRR = & -587.4722 + 5.0316T_{ON} + 4.2548T_{OFF} \\ & + 31.4766IP + 0.3222SV - 0.0089T_{ON}T_{OFF} \\ & + 0.1422T_{ON}IP - 0.00079T_{ON}SV \\ & - 0.0797T_{OFF}IP - 0.0001T_{OFF}SV \\ & - 0.02179IPSV - 0.02676T_{ON}^2 \\ & - 0.0225T_{OFF}^2 - 1.7985IP^2 - 0.00015\,SV^2 \quad (12) \end{aligned}$$

Table 6. ANOVA and *F*-test for kerf.

Serial number	Process parameters	Degrees of freedom	Sum of squares	Mean square	*F*-test	*p*-value (prob > *F*)	Percentage of contribution
1	A—T_{ON}	1	0.003641	0.003641	20.04407	0.0009	10.61349
2	B—T_{OFF}	1	0.000338	0.000338	1.860781	0.1998	0.985298
3	C—IP	1	0.010609	0.010609	58.40754	< 0.0001	30.92724
4	D—SV	1	0.008235	0.008235	45.33436	< 0.0001	24.00489
5	AB	1	0.00087	0.00087	4.790961	0.0511	2.536851
6	AC	1	0.00297	0.00297	16.35203	0.0019	8.658524
7	AD	1	0.00038	0.00038	2.093379	0.1758	1.10846
8	BC	1	4.23E-05	4.23E-05	0.232598	0.6391	0.123162
9	BD	1	0.000132	0.000132	0.728072	0.4117	0.38552
10	CD	1	0.00024	0.00024	1.322641	0.2745	0.700349
11	A^2	1	0.00022	0.00022	1.211929	0.2945	0.641726
12	B^2	1	7.65E-06	7.65E-06	0.042127	0.8411	0.022306
13	C^2	1	0.000902	0.000902	4.967967	0.0476	2.630577
14	D^2	1	0.000117	0.000117	0.646464	0.4384	0.342308
15	Residual	11	0.001998	0.000182			
16	Lack of fit	10	0.001986	0.000199	15.88469	0.1930	5.788146
17	Pure error	1	1.25E-05	1.25E-05			0.036439
18	Cor. total	25	0.034304				100

T_{ON}: pulse-on time; T_{OFF}: pulse-off time; IP: peak current; SV: servo voltage; Cor. total: Corrected Total.

ANOVA results for SR are listed in Table 5. It can be observed that the IP, SV, $T_{ON}\times$ SV, IP $\times$ SV and IP^2 are the most significant factors. The R^2 is given as 0.9066 and adjusted R^2 is 0.7877. Regression equation for SR is given in equation (13)

$$\begin{aligned} SR = {} & 358.0665 - 4.2843T_{ON} - 0.7267T_{OFF} \\ & - 19.1883IP + 0.3485SV + 0.0022T_{ON}T_{OFF} \\ & + 0.0125T_{ON}IP \\ & - 0.00203T_{ON}SV - 0.02575T_{OFF}IP \\ & + 0.0007T_{OFF}SV - 0.0157IPSV \\ & + 0.01884T_{ON}^2 + 0.00644\,T_{OFF}^2 \\ & + 0.871IP^2 + 0.00019SV^2 \end{aligned} \quad (13)$$

ANOVA results for kerf are listed in Table 6. The significant parameters are T_{ON}, IP, SV, T_{ON} X IP and IP^2. The R^2 is given as 0.9418 and adjusted R^2 is 0.8676. Regression equation for kerf is given by equation (14)

$$\begin{aligned} kerf = {} & - 1.3977 + 0.03701T_{ON} - 0.04204T_{OFF} \\ & + 0.11478IP - 0.00199SV + 0.0003T_{ON}T_{OFF} \\ & + 0.00272T_{ON}IP + 2.4375E - 05T_{ON}SV \\ & + 0.0003T_{OFF}IP - 0.00001T_{OFF}SV \\ & + 9.6875E - 05IPSV \\ & - 0.00037T_{ON}^2 + 6.91429E - 05T_{OFF}^2 \\ & - 0.01877IP^2 - 4.23214E - 06SV^2 \end{aligned} \quad (14)$$

Results and discussion

FA is implemented using MATLAB software. The algorithm is tested with different population sizes and found that beyond the population size of 20 fireflies, there was no much variation in solution convergence. Population size of 20 fireflies is used, and 500 iterations are performed. Individual optimization of MRR using FA yields a maximum of 8.967 mm^3/min at T_{ON} (115 μs), pulse-off time (T_{OFF}) (50 μs), IP (12 A) and SV (10 V), as presented in Table 7. It is observed that maximum MRR is predicted at high IP, low SV and high pulse-on time (T_{ON}). This is because, strong sparks are generated at higher IPs and low SV. Higher pulse-on time ensures to hold energy for longer duration of time, producing high temperature. As a result, more material is melted and eroded. Figure 3 shows the convergence plot of MRR and the solution is converged at 12^{th} iteration.

Individual optimization of SR using FA yields a minimum value of 1.136 μm at T_{ON} (107 μs), T_{OFF} (60 μs), IP (11 A) and SV (10 V). It is observed that IP and SV play a vital role in minimizing SR. With increased IP, intense energy will be generated forming a deeper crater causing higher SR. However, from the ANOVA, it is evident that interaction effect of IP and SV is also significant on the SR. Also, better SR is observed at low SV. This is because interelectrode gap at low SV is much narrow keeping the wire much closer to the workpiece. This helps to machine the peaks on the material, thereby minimizing the SR. Convergence is observed at 14^{th} iteration, as shown in Figure 3.

Individual optimization of kerf yields 0.298 mm at T_{ON} (115 μs), T_{OFF} (50 μs), IP (10 A) and SV (10 V). For minimizing the kerf, IP and SV are important. At lower IP and SV, spark energy is less forming smaller size debris. These debris are easy to evacuated from the machining zone, thereby resulting in low kerf. If the debris size is larger, evacuation becomes difficult. It can result in multiple sparks, which can widen the kerf. The convergence plot for kerf is shown in Figure 4. The solution is obtained at 42^{nd} iteration.

Table 7. Results of firefly algorithm for individual responses.

Response parameters	Optimized machining parameters				Objective function
	T_{ON} (μs)	T_{OFF} (μs)	IP (A)	SV (V)	
MRR (mm^3/min)	115	50	12	10	8.967
SR (μm)	107	60	11	10	1.136
Kerf (mm)	115	50	10	10	0.298

T_{ON}: pulse-on time; T_{OFF}: pulse-off time; IP: peak current; SV: servo voltage; MRR: material removal rate; SR: surface roughness.

Table 8. Results of multiobjective optimization using GRA coupled with FA.

Optimized machining parameters				Multiobjective function		
T_{ON} (μs)	T_{OFF} (μs)	IP (A)	SV (V)	MRR	SR	Kerf
109	55	12	52	6.2	1.49	0.36

T_{ON}: pulse-on time; T_{OFF}: pulse-off time; IP: peak current; SV: servo voltage; MRR: material removal rate; SR: surface roughness.

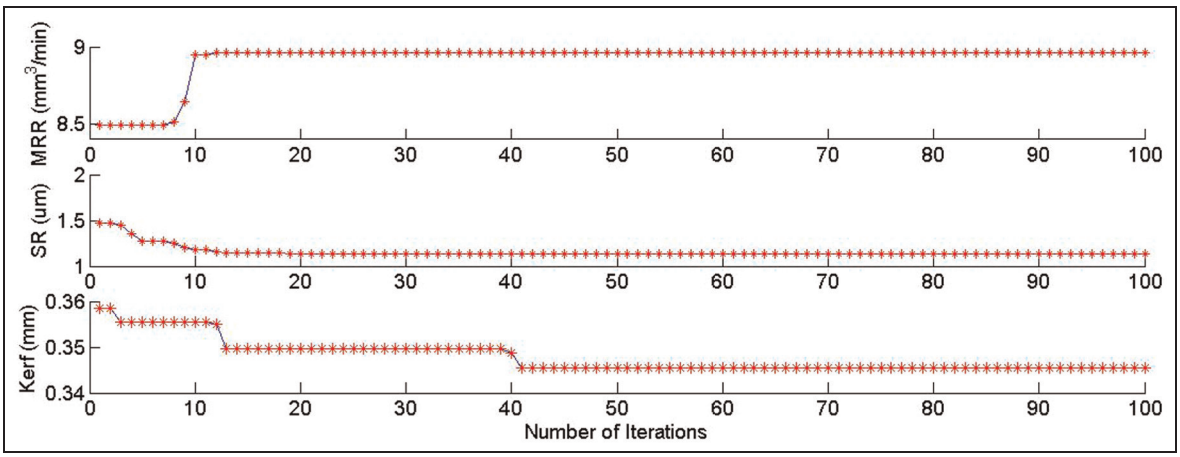

Figure 3. Convergence plot for MRR, SR and kerf.
MRR: material removal rate; SR: surface roughness.

Simultaneous optimization of three responses using the proposed GRA coupled with FA method yields MRR of 6.2 mm^3/min, SR of 1.49 μm and kerf of 0.36 mm. The corresponding process parameters observed are T_{ON} (109 μs), T_{OFF} (55 μs), IP (12 A) and SV (52 V), as presented in Table 8. It is evident from the ANOVA that IP has the most dominant influence on MRR, SR and kerf. Hence, this parameter will have the most influencing effect when considered simultaneously also. Higher IP causes MRR to increase while compromising on SR and kerf. However, due to the effects of other process parameters and their interactions, global optimal solution for the simultaneous optimization of multiple objectives is obtained almost at the middle levels of the process parameters. At these levels, narrow interelectrode gap results in much focused plasma channel, which increases volume of material removed per spark with larger crater. As a result, increase in MRR and SR is observed. kerf decreases with narrow interelectrode gap. In the proposed optimization strategy, process parameters are tuned for achieving the best possible compromise among the responses. Simultaneous optimal point is obtained at 49th iteration, as shown in Figure 4.

When there are two or more objectives with conflicting interests, solution rarely exists optimizing all the objectives simultaneously. Ming et al.[19] suggested a Pareto optimal front for triple objective optimization of WEDM. It was observed that if good surface finish is required, a compromise on MRR is required and vice versa. Hence, these Pareto plots were found to be helpful in understanding the trend of solution set. In this work, 50 solution sets are obtained by repeating the program execution. The objectives are taken along the three axes of the three-dimensional (3D) Pareto surface plot, as shown in Figure 5. Figure 6 shows the contour plot of Figure 5. Each bubble describes a solution. The point "B_1" in Figures 5 and 6 describes a solution at which MRR is maximum. However, SR and kerf are not minimum. Similarly, point "B_2" is a solution of

minimum SR and kerf. This point does not give maximum MRR. Solutions such as point A in Figures 5 and 6 are said to be dominated by others. Solutions such as B_1, B_2, …, B_n have the characteristic that no other solution, which satisfies all the three objectives, simultaneously exists. These are said to be non-dominated solutions. The line or surface on which these solutions lie is called non-dominated or optimum trade-off line or surface. The objective function values corresponding to the non-dominated set of solutions are called the Pareto set. The trade-off surface identifies the subset of solutions that offer the best compromise among the objectives.

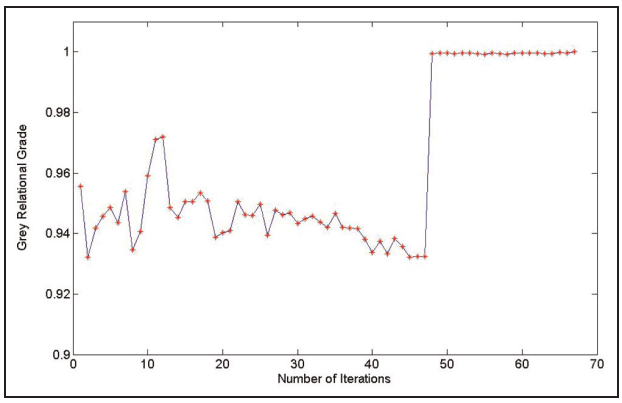

Figure 4. Convergence plot of GRA coupled with FA for multiobjective optimization of MRR, SR and kerf.

Conclusion

Manufacturing sector has always been practicing compromise among the output responses. In the case of WEDM, because of the stochastic nature of the process, exploring multiobjective optimal machining parameters has become difficult. From the literature, FA was found to be superior to other algorithms when tested on benchmark problems. This work also exploits the accuracy and fast convergence offered by FA. However, this algorithm can optimize a single response at a time. WEDM being a multiobjective problem, a novel optimization strategy is proposed in this work by coupling the FA with GRA. GRA is used in FA for combining multiple objectives into a single GRG. This grade is used for the movement of a firefly to the brighter and

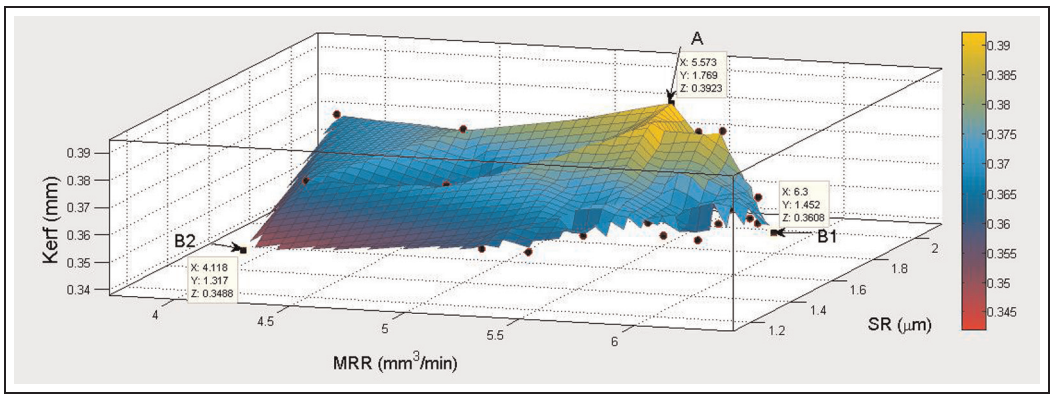

Figure 5. 3D Pareto surface plot for the responses.
MRR: material removal rate; SR: surface roughness.

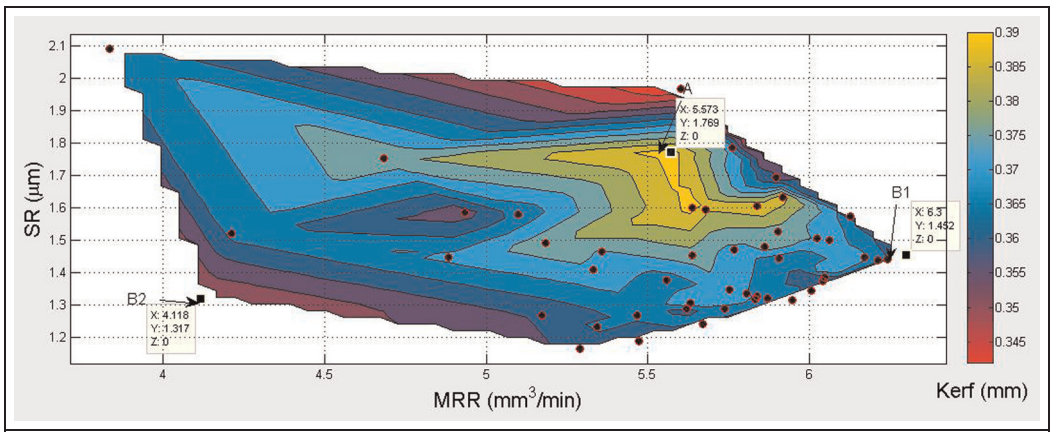

Figure 6. Contour plot of responses.
MRR: material removal rate; SR: surface roughness.

attractive firefly. In this process, a simultaneous optimal solution for MRR, SR and kerf is obtained within the selected machining parameters.

IP is found to be the most influencing factor affecting all the three responses MRR, SR and kerf. Pareto surface and contour plots are also plotted to recommend alternate solutions for selection of responses based on the priorities. Since the proposed strategy is generalized, it can easily be customized for other multi-objective optimization problems also.

Declaration of conflicting interests

The authors declare that there is no conflict of interest.

Funding

This research received no specific grant from any funding agency in the public, commercial or not-for-profit sectors.

References

1. Golshan A, Ghodsiyeh D and Izman S. Multi-objective optimization of wire electrical discharge machining process using evolutionary computation method: effect of cutting variation. *Proc IMechE, Part B: J Engineering Manufacture*. Epub ahead of print 20 March 2014. DOI: 10.1177/0954405414523593.
2. Rao RV and Pawar PJ. Modelling and optimization of process parameters of wire electrical discharge machining. *Proc IMechE, Part B: J Engineering Manufacture* 2009; 223: 1431–1440.
3. Garg MP, Jain A and Bhushan G. Modelling and multi-objective optimization of process parameters of wire electrical discharge machining using non-dominated sorting genetic algorithm-II. *Proc IMechE, Part B: J Engineering Manufacture* 2012; 226: 1986–2001.
4. Yang X-S. *Engineering optimization: an introduction with metaheuristic applications*. New York: Wiley, 2010.
5. Yang X-S. *Nature-inspired metaheuristic algorithms*. Beckington: Luniver Press, 2008.
6. Yang X-S. Firefly algorithms for multimodal optimization. In: Watanabe O and Zeugmann T (eds) *Stochastic algorithms: foundations and applications* (SAGA 2009: LNCS, vol. 5792). Berlin, Heidelberg: Springer, 2009, pp.169–178.
7. Khadwilard A, Chansombat S, Thepphakorn T, et al. Application of firefly algorithm and its parameter setting for job shop scheduling. *J Ind Tech* 2012; 8(1): 1–10.
8. Aungkulanon P, Chai-ead N and Luangpaiboon P. Simulated manufacturing process improvement via particle swarm optimization and firefly algorithm. In: *Proceedings of the international multi-conference of engineers and computer scientists*, vol. II, Hong Kong, 16–18 March 2011.
9. Bharathi Raja S, Sathiya Narayanan N, Srinivas Pramod CV, et al. Optimization of constrained machining parameters in turning operation using firefly algorithm. *J Appl Sci* 2012; 12(10): 1038–1042.
10. Chai-ead N, Aungkulanon P and Luangpaiboon P. Bees and firefly algorithms for noisy non-linear optimization problems. In: *Proceedings of the international multi-conference of engineers and computer scientists*, vol. II, Hong Kong, 16–18 March 2011.
11. Bharathi Raja S, Srinivas Pramod CV, Vamshee Krishna K, et al. Optimization of electrical discharge machining parameters on hardened die steel using firefly algorithm. *Eng Comput*. 2013. DOI: 10.1007/s00366-013-0320-3.
12. Apostolopoulos T and Aristidis V. Application of the firefly algorithm for solving the economic emissions load dispatch problem. *Int J Comb* 2011; 2011: 523806 (23 pp.).
13. Lin K-W and Wang C-C. Optimizing multiple quality characteristics of wire electrical discharge machining via Taguchi method-based gray analysis for magnesium alloy. *J CCIT* 2010; 39(1): 23–34.
14. Wolpert DH and Macready WG. No free lunch theorems for optimization. *IEEE T Evolut Comput* 1997; 1(1): 67–82.
15. Yang X-S. Multiobjective firefly algorithm for continuous optimization. *Eng Comput* 2013; 29: 175–184.
16. Deng JL. Introduction to grey system. *J Grey Syst* 1989; 1: 1–24.
17. Kaluri RS and Basak T. Entropy generation due to natural convection in discretely heated porous square cavities. *Energy* 2011; 36(8): 5065–5080.
18. Chen Y and Qu L. Evaluating the selection of logistics centre location using fuzzy MCDM model based on entropy weight. In: *Proceedings of the 6th world congress on intelligent control and automation*, Dalian, China, 21–23 June 2006. New York: IEEE.
19. Ming W, Zhang Z, Zhang G, et al. Multi-objective optimization of 3D-surface topography of machining YG15 in WEDM. *Mater Manuf Process* 2014; 29: 514–525.